Polydimethylsiloxane (PDMS)-based Giant Glycosylated Polymersomes with Tuneable Bacterial Affinity

Liam Martin,[1] Pratik Gurnani,[1] Junliang Zhang,[1] Matthias Hartlieb,[1] Neil R. Cameron,[2,3] Ahmed M. Eissa[1,2,4] and Sébastien Perrier[1,5,6*]*

[1] Department of Chemistry, University of Warwick, Coventry CV4 7AL, United Kingdom.

[2] School of Engineering, University of Warwick, Coventry CV4 7AL, U.K.

[3] Department of Materials Science and Engineering, Monash University, Clayton, VIC 3800, Australia.

[4] Department of Polymers, Chemical Industries Research Division, National Research Centre (NRC), El-Bohouth Street, Dokki, 12622, Cairo, Egypt.

[5] Warwick Medical School, University of Warwick, Coventry CV4 7AL, U.K.

[6] Faculty of Pharmacy and Pharmaceutical Sciences, Monash University, VIC 3052, Australia.

* a.m.eissa@warwick.ac.uk; s.perrier@warwick.ac.uk

A synthetic cell mimic in the form of giant glycosylated polymersomes (GGPs) comprised of a novel amphiphilic diblock copolymer is reported. A synthetic approach involving a poly(dimethylsiloxane) (PDMS) macro-chain transfer agent (macroCTA) and post-polymerization modification was used to marry the hydrophobic and highly flexible properties of PDMS with the biological activity of glycopolymers. 2-Bromoethyl acrylate (BEA) was first polymerized using a PDMS macroCTA ($M_{n,th}$ ≈ 4900 g.mol^{-1}, $Đ$ = 1.1) to prepare well-defined PDMS-*b*-pBEA diblock copolymers ($Đ$ = 1.1) which were then substituted with 1-thio-*β*-D-glucose or 1-thio-*β*-D-galactose under facile conditions to yield PDMS-*b*-glycopolymers. Compositions possessing ≈ 25 % of the glycopolymer block (by mass) were able to adopt a vesicular morphology in aqueous solution (≈ 210 nm in diameter) as indicated by TEM and light scattering techniques. The resulting carbohydrate-decorated polymersomes exhibited selective binding with the lectin concanavalin A (Con A) as demonstrated by turbidimetric experiments. Self-assembly of the same diblock copolymer compositions using an electroformation method yielded GGPs (ranging from 2 – 20 μm in diameter). Interaction of these cell-sized polymersomes with *fim*H positive *E. coli* was then studied *via* confocal microscopy. The glucose-decorated GGPs were found to cluster upon addition of the bacteria, while galactose-decorated GGPs could successfully interact with (and possibly immobilize) the bacteria without the onset of clustering. This demonstrates an opportunity to modulate the response of these synthetic cell mimics (protocells) towards biological entities through exploitation of selective ligand-receptor interactions, which may be readily tuned through a considered choice of carbohydrate functionality.

Introduction

Cells are tremendously complex entities, the site of innumerable vital biological functions, and as such the mimicry of cellular structure and function *via* synthetic means is a highly appealing prospect. However, reproducing such complexity currently remains well beyond scientific capability. As such the present goal is to instead develop compartments structurally reminiscent of biological cells, termed protocells, which can perform one or more biological functions.[1-6] Numerous examples of primitive synthetic cell models exploring different aspects of cellular function such as metabolism,[7-8] growth[9-10] and division[9, 11] have been reported using a range of synthetic approaches.

In recognition of the supramolecular composition of cellular membranes, many protocell models are based on supramolecular assemblies of amphiphilic building blocks, either naturally-derived or wholly synthetic. Liposomes offer the most immediately comparable cell membrane models on a structural level since they are also typically comprised of low molar mass (< 1 kDa) phospholipids and have therefore been used extensively.[12-17] However, a variety of non-lipidic synthetic building blocks have also been employed to prepare protocell models, including protein-polymer nano-conjugates,[18] polypeptides[19] and block copolymers.[3] Amphiphilic block copolymer vesicles (polymersomes) represent an appealing candidate as protocell models by virtue of the expansive chemical variety which can be accessed, offering the opportunity to control structural, mechanical and biological properties of the resultant polymersome membrane.[20-23] Amphiphilic block copolymers are often referred to as "super" amphiphiles since they are of substantially higher molar mass than phospholipids, and as such polymersomes possess thicker bilayer membranes than liposomes.[24] While an increased membrane thickness typically corresponds to superior colloidal stability, it translates to a decrease in membrane fluidity and permeability. Indeed, the relationship between block copolymer molar mass and membrane properties such as membrane thickness, rigidity and permeability has been demonstrated.[25-26]

Amphiphilic block copolymers containing a hydrophobic segment with a low glass transition temperature (T_g), such as poly(dimethylsiloxane) (PDMS), can generate "fluid" polymeric membranes with mechanical properties approaching those of natural membranes despite being substantially thicker.[27] It has been found that ABA triblock copolymers consisting of two outer poly(2-

methyloxazoline) (PMOXA) blocks and a PDMS middle block (PMOXA-PDMS-PMOXA) which self-assemble to form vesicles are excellent for the reconstitution of membrane proteins and membrane channel proteins.[28-33] Remarkably, the functionality of the reconstituted proteins was fully preserved, under a critical membrane thickness of 9.2 – 12.1 nm, despite their artificial host.[34] Such an approach could be adopted for the preparation of a polymeric protocell model using amphiphilic block copolymers whereby the hydrophobic block contributes towards a "fluid" membrane structure while the hydrophilic block may be exploited to impart biological function *via* presentation of relevant chemical functionalities.

One crucial property exhibited by cells is the ability to recognize, and interact with, their surroundings. This is possible due to the architecture of the cell membrane, a semipermeable supramolecular barrier which hosts a diverse variety of functional macromolecules. Such an array of complex surface chemistries permits discrimination between extracellular species, provoking an appropriate cellular response, a feature which the scientific community strives to mimic.[35-38] Carbohydrates are structurally complex molecules which can participate in highly specific ligand-receptor interactions with lectins (cell surface carbohydrate-binding proteins). The "docking" of carbohydrate-bearing cargo to the cell surface through such selective binding is an initial step in a number of biological functions such as fertilization, inflammation, virus docking and receptor-mediated endocytosis (RME).[39-41] Carbohydrates are also readily derivatizable and as such glycosylated materials are often exploited by synthetic chemists as a targeting moiety.[42-48] To this end, a number of supramolecular architectures such as micelles, worm-like micelles and vesicles have been formed from a variety of glycosylated amphiphilic building blocks, which have been demonstrated to bind selectively with lectins.[49-51] Pasparakis and Alexander reported the preparation of large sub-micron polymersomes displaying glucose residues on the surface from a doubly hydrophilic poly(2-glucosyloxyethyl methacrylate)-*block*-poly(diethyleneglycol methacrylate) (pDEGMA-*b*-pGEMA) copolymer made *via* reversible deactivation radical polymerization (RDRP) methods.[52] These polymersomes were able to undergo selective binding with a GFP fluorescent *E. coli* strain expressing the *fim*H membrane receptor, which possesses high binding affinities for glucose and mannose, and furthermore it was demonstrated

that this specificity could be exploited to transfer small molecule "information" in the event of binding. Kubilis *et al.* reported a glycosylated giant polymersome protocell model made from amphiphilic poly(glucosyloxyethyl acrylamide)-*block*-poly(butyl acrylate) (pGEAm-*b*-pBA) synthesised *via* RAFT polymerization.[53] Selective binding between the micron-scale, glucose-decorated polymersomes and fluorescent polystyrene beads functionalized with the lectin Concanavalin A (Con A), representing virus particles, was observed using confocal microscopy. Glycosylated nanoparticles are also promising materials in anti-adhesion therapy, since their lectin-binding with bacterial membranes can interfere with the binding between bacteria and mammalian cell membranes in the early stages of infection.[54]

Previous comparative studies of membrane properties of liposomes and polymersomes determined by atomic force microscopy imaging and force spectroscopy showed that poly(dimethylsiloxane)-based polymersomes display a Young's modulus of 17 ± 11 MPa and a bending modulus of 70 ± 50 × 10^{-19} J which are much closer to typical values for lipids in the gel-phase such as dipalmitoylphosphatidylcholine (110 ± 15 MPa and 14 ± 2 × 10^{-19} J, respectively) than those for other types of polymersomes such as polystyrene-based polymersomes (61 ± 6 MPa and 716 ± 103 × 10^{-19} J, respectively).[27, 55-56] We therefore aimed to build upon these examples by designing a polymeric protocell model with a novel membrane composition, which possesses mechanical properties closer to that of a natural vesicular membrane and may "recognize" certain extracellular species *via* selective carbohydrate-lectin binding. Herein we report the development of a new amphiphilic block copolymer consisting of an extremely low T_g poly(dimethylsiloxane) hydrophobic segment and a glycopolymer hydrophilic segment prepared using a macro-chain transfer agent (macro-CTA), RAFT polymerization and post-polymerization modification approach. The self-assembly behavior and subsequent lectin-binding potential of these novel block copolymers was first studied on the nano-scale using a solvent switch approach and turbidimetric experiments with ConA. These concepts were then translated to the micro-domain, using the block copolymers to form giant glycosylated polymersomes and studying their binding behavior with *fim*H positive *E. coli*.

Results and Discussion

The synthetic approach utilized for the preparation of the desired amphiphilic PDMS-*b*-glycopolymer structures entailed the synthesis of a PDMS macroCTA followed by RAFT polymerization to give the reactive PDMS-*b*-poly(2-bromoethyl acrylate) (PDMS-*b*-PBEA) precursor, and finally the nucleophilic substitution of the pendant bromine groups with 1-thio carbohydrate derivatives, as shown in Scheme 1. RAFT polymerization was to synthesize these materials since it is very versatile and robust RDRP method, capable of controlling molar mass and molar mass distributions for a wide range of functional vinyl monomers.[57-59] The macroCTA approach has previously been demonstrated to work well to obtain PDMS-containing block copolymers.[58, 60-64]

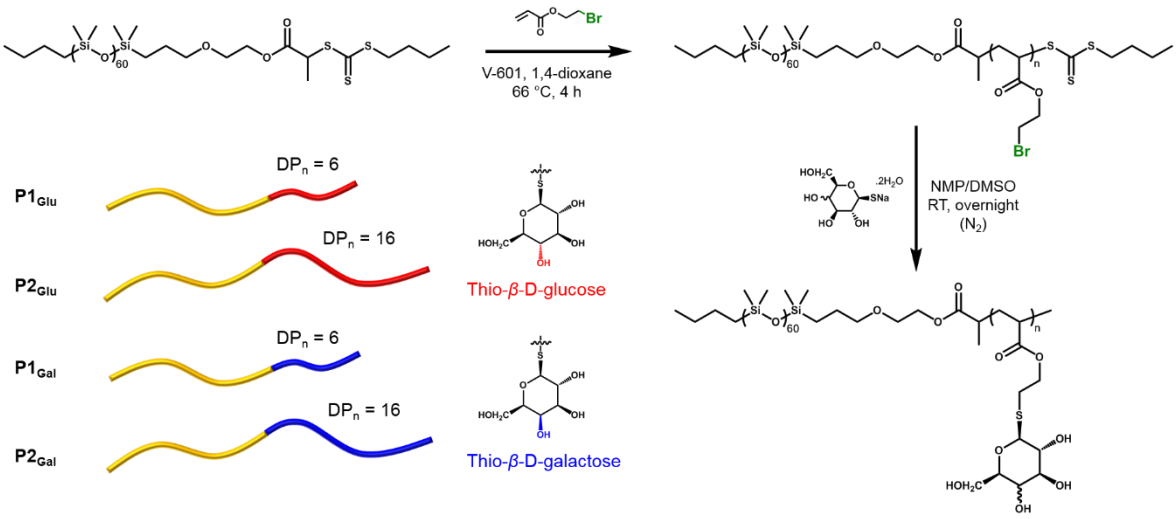

Scheme 1. Synthetic approach for the preparation of well-defined amphiphilic PDMS-Glycopolymer diblock copolymers.

The post-modification approach is appealing since a single well-defined precursor polymer can be used to prepare a range of functional polymers (e.g. possessing different carbohydrates) with the same degree of polymerization (DP_n) and molar mass distribution ($Đ$). Glycopolymers have been successfully generated using a range of post-polymerization reactions including copper catalyzed azide-alkyne cycloadditions, thiol-ene and thiol-yne "click" reactions, nucleophilic activated ester/amine

exchange and nucleophilic substitution.[65] Recently, thio-bromo substitutions of alkyl-bromine containing precursors have been demonstrated as an efficient route towards well-defined glycopolymers.[66-67] Barlow *et al.* reported the preparation of a wide range of functional RAFT polymers, including a glycopolymer, *via* nucleophilic substitution of well-defined poly(bromoethyl acrylate) precursors.[66] These substitutions were quantitative in most cases and could be conducted under facile conditions, whilst substitution with 1-thio-*β*-D-glucose yielded a glycopolymer with a narrow molar mass distribution ($Đ$ < 1.2). Pröhl *et al.* used this substitution to prepare relatively high molar mass (≈ 35,000 g.mol^{-1}) glycopolymers bearing a variety of different carbohydrates.[67] We postulated that this thio-bromo nucleophilic substitution could be exploited to prepare well-defined PDMS-*b*-glycopolymer with a composition promoting self-assembly in aqueous solution into glycosylated polymersomes.

Synthesis of PDMS macroCTA

The PDMS-((propanoate) butyl trithiocarbonate) (PDMS-PBTC) macroCTA was prepared using an EDCI/DMAP catalyzed esterification between (propanoic acid)yl butyl trithiocarbonate (PABTC) and the commercially available monohydroxy terminated PDMS (average M_n ≈ 4670 g.mol^{-1}) (PDMS-OH) in accordance with a previously reported procedure and was characterized using ^{1}H NMR spectroscopy and size exclusion chromatography (SEC).[60] Successful esterification was confirmed by ^{1}H NMR spectroscopy, with the peak at 3.74 ppm (-*CH*$_2$-OH) shifting to 4.29 ppm (-*CH*$_2$-(O)O-) (Fig. S1). Furthermore, integration of the peak at 3.42 ppm (-S-*CH*$_2$-CH$_2$-) and 4.29 ppm (-*CH*$_2$-(O)O-) confirmed quantitative esterification. THF-SEC of the PDMS-OH precursor and the PDMS-PBTC macro-CTA each possessed monomodal populations with narrow molar mass distributions ($Đ$ < 1.1). The experimental molar mass obtained was substantially higher than theoretical values which can be attributed to the difference in hydrodynamic volume between PDMS and the poly(methyl methacrylate) narrow standards used for SEC calibration (Table 1).

RAFT polymerization of 2-bromoethyl acrylate using PDMS-PBTC macro-CTA

RAFT polymerizations of 2-bromoethyl acrylate using the PDMS-PBTC macroCTA were conducted in 1,4-dioxane using dimethyl 2,2'-azobis(2-methylpropionate) (V-601) as initiator (Scheme 1). Two diblock copolymer compositions were targeted whereby the final PDMS-*b*-glycopolymers would (theoretically) possess 25 % or 50 % glycopolymer (by mass), assuming complete substitution of the pendant bromine groups by 1-thio-*β*-D-glucose or 1- thio-*β*-D-galactose. It was expected that these compositions would exhibit different self-assembly behavior in aqueous media, with the former adopting a vesicular morphology and the latter forming micelles, or possibly worm-like micelles.[68-70] The concentration of monomer and initiator were fixed for each polymerization ($[BEA]_0$ = 0.55 mol.L^{-1}, $[V\text{-}601]_0$ = 2.5 × 10^{-3} mol.L^{-1}) and each polymerization was left at 66 °C for 4 h, while the concentration of PDMS-PBTC was varied to target different degrees of polymerization (DP_n) for the PBEA block. The polymerizations were stopped at moderate monomer conversions (< 70 %) in order to reduce the occurrence of termination events and other side reactions. The degree of polymerization and theoretical molar mass of the purified polymers were determined using ^{1}H NMR spectroscopy by comparing the integrals of the peak(s) at 0.4 –0.5 ppm (4 protons, assigned d and f in Fig. 1b) with the peaks at 3.4 – 3.6 ppm (assigned z and i).

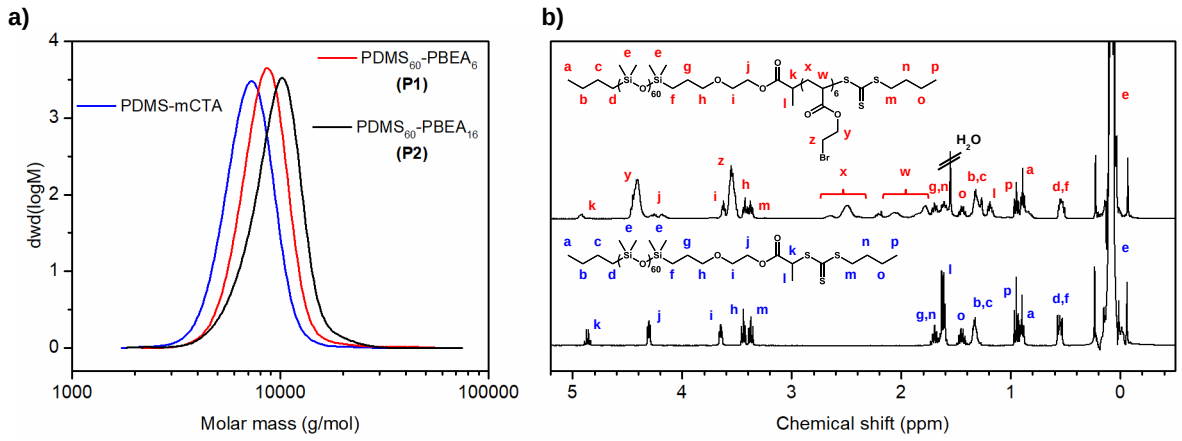

Figure 1. THF-SEC chromatograms of PDMS-PBTC macroCTA and purified $PDMS_{60}$-*b*-PBEA polymers following 4 h of RAFT polymerization at 66 °C in 1,4-dioxane **(a)**. ^{1}H NMR spectra ($CDCl_3$) of the $PDMS_{60}$-PBTC macroCTA and purified $PDMS_{60}$-*b*-$PBEA_6$ **(P1)** following 4 h of RAFT polymerization at 66 °C in 1,4-dioxane **(b)**.

$PDMS_{60}$-*b*-$PBEA_n$ diblock copolymers with $DP_{n,(BEA)}$ of ≈ 6 and ≈ 16 (**P1** and **P2**, respectively**)** were obtained following precipitation in MeOH/H_2O. THF-SEC revealed monomodal populations with a clear shift towards higher molar mass from the initial PDMS-PBTC macroCTA (Fig. 1a and Table 1) and narrow molar mass distributions ($Đ$ < 1.1) indicating the RAFT polymerization proceeded in a controlled manner. The block copolymers were also characterized using differential scanning calorimetry (DSC) (Fig. S8 and S9, supporting information). The glass transition (T_g ~ -125 °C), cold crystallization transition (T_c ~ -88 °C) and melting transition (T_m ~ -50 °C) typically attributed to PDMS were all observed.[60] Finally, elemental analysis of the purified polymers was consistent with the predicted structures and indicate retention of the pendant bromine group (Table S1 in supporting information) following RAFT polymerization.

Table 1. Summary of $PDMS_{60}$-*b*-pBEA diblock copolymers prepared *via* RAFT polymerization with the PDMS-PBTC macroCTA.

Entry	Composition	$DP_{n,(BEA)}$ (target)	$DP_{n,(BEA)}$ (NMR)[a]	($g.mol^{-1}$) $M_{n,th}$	$M_{n,SEC}$	$Đ_{SEC}$
1	**PDMS-PBTC**	-	-	4900	6750	1.08
2[b] (P1)	**$PDMS_{60}$-*b*-$PBEA_6$**	10	6	5950	8050	1.09
3[b] (P2)	**$PDMS_{60}$-*b*-$PBEA_{16}$**	25	16	7750	9050	1.10

SEC performed in THF using PMMA narrow standards for calibration.

[a] Determined from ^1H NMR data.

[b] Polymerization conditions: $[BEA]_0$ = 0.55 $mol.L^{-1}$, $[V\text{-}601]_0$ = 2.5 $mmol.L^{-1}$, 4 h at 66 °C.

Post-polymerization substitution

Following the synthesis of the precursor $PDMS_{60}$-*b*-$PBEA_n$ diblock copolymers **P1** and **P2**, the pendant bromine groups were substituted with either 1-thio-*β*-D-glucose or 1-thio-*β*-D-galactose to generate the desired amphiphilic diblock copolymers $PDMS_{60}$-*b*-P(*Glu*EA)$_n$ (**$P1_{Glu}$** and **$P2_{Glu}$**) and $PDMS_{60}$-*b*-P(*Gal*EA)$_n$ (**$P1_{Gal}$** and **$P2_{Gal}$**). Since the thio-sugars were purchased in their sodium salt forms, no additional base was required to facilitate the nucleophilic substitution. For substitution of the precursor copolymers, a solvent system of DMSO and *N*-methyl-2-pyrrolidone (NMP) (35/65 by volume, respectively) was used. This solvent system was selected since it is both aprotic and relatively polar, to allow for an efficient S_N2 substitution, and moreover was able to readily solubilize both the hydrophobic precursor polymer and the hydrophilic thio-sugar. A two-fold excess of thio-sugar with respect to bromine moieties was employed to ensure complete substitution. The resulting substituted polymers were obtained in high yields (> 85 %) following purification *via* dialysis and lyophilization. Heteronuclear single quantum correlation (HSQC) spectroscopy experiments were instrumental in characterization of the substituted polymers (Fig. S2 – S7, supporting information). Following modification, the peak at δ(^1H,^{13}C): 3.50, 28.64 ppm corresponding to the CH_2 adjacent to the bromine pendant group (CH_2-*CH_2*-Br) disappears and is replaced with new peaks at δ(^1H,^{13}C): 2.70 – 2.90, 27.94 ppm attributed to the new CH_2-*CH_2*-S- species. Additionally, peaks corresponding to the new thio-sugar pendant groups are observed which indicate successful substitution (assigned 1-6 in Fig. S4 – 7).

Finally, the peaks corresponding to the ω-chain end of the polymers (assigned m-p in Fig. 1b and Fig. S2/3) are no longer observed indicating loss of the RAFT end group, which is unsurprising since the nucleophilic thio-sugar anion (which is used in excess) may also undergo nucleophilic addition to the trithiocarbonate moiety, yielding free thiol ω-chain ends. As a result it is possible that some disulphide bonds form following exposure to air, either between two ω-chain ends or between ω-chain end and excess thiosugar, yielding a BAB triblock copolymer or an AB diblock copolymer with an additional thioglucose at the ω-chain end, respectively. DSC of the substituted polymers reveals a loss of T_m (Fig. S8/9). This is potentially due to the influence of the glycopolymer block on the molecular packing which may hinder the crystallization of PDMS. With the substituted **P1** polymers (**P1$_{Glu}$** and **P1$_{Gal}$**) no thermal transition corresponding to the T_g of the new glycopolymer block could be identified due to the low molar mass of this block (Fig. S8). However for the substituted **P2** polymers a new T_g attributed to glycopolymer blocks are observed at 82 °C and 80 °C for **P2$_{Glu}$** and **P2$_{Gal}$**, respectively (Fig. S9). Elemental analysis of the purified polymers confirmed complete loss of bromine following substitution whilst the content of carbon and hydrogen increase slightly in close agreement with the predicted structure (Table S1 in supporting information), indicating quantitative substitution. Interestingly, for substitution of **P1** and **P2** with 1-thio-β-D-galactose it was necessary to work at substantially greater dilution (two-fold compared to when 1-thio-β-D-glucose was used) to ensure both the PDMS-*b*-PBEA precursors and thio-galactose remained in solution, also necessitating the introduction of a small amount of water (3 % by volume) to facilitate solubilization of the thio-sugar. Nevertheless, **P1$_{Gal}$** and **P2$_{Gal}$** were still obtained in high yields, and successful substitution was confirmed.

Polymersome formation and binding with Con A

The self-assembly behaviour of these novel well-defined amphiphilic glycopolymers was investigated. **P1$_{Glu}$** and **P1$_{Gal}$**, possessing a high hydrophobic content (approximately 75 % by mass), were expected to adopt a vesicular morphology. Meanwhile **P2$_{Glu}$** and **P2$_{Gal}$**, theoretically possessing 50 % hydrophobic content (by mass), were expected to self-assemble to give micelles or worm-like micelles.[20, 23, 69, 71] However, it is recognized that the adopted morphology of block copolymer self-

assemblies is determined by a number of factors which dictate the packing behavior of the polymeric blocks, and not simply the hydrophobic/hydrophilic mass ratio.[68] Moreover, the self-assembly process employed can have a strong influence on the final morphology obtained.[69, 72]

A simple solvent-switch method from an initial THF/MeOH solution (95:5) to water was employed with **P1$_{Glu}$** and **P1$_{Gal}$** to induce self-assembly in water. The subsequent suspensions (which were turbid at a concentration of 2 mg.mL^{-1}) were studied by dynamic light scattering (DLS) and static light scattering (SLS). DLS measurements revealed the presence of monomodal populations possessing an average hydrodynamic diameter (D_h) of ≈ 210 and 220 nm for **P1$_{Glu}$** and **P1$_{Gal}$**, respectively, and polydispersity indices (PDI) of 0.1 or below (Table 2, Fig. 2b, S10 and S11). The average apparent molar mass (M_a) and aggregation number (N_{agg}) of the self-assemblies was determined by SLS using an Ornstein-Zernicke representation of the scattering data (Table 2 and Fig. S12). Considering the structural similarity of **P1$_{Glu}$** and **P1$_{Gal}$** and (theoretically) equal molar mass (approximately 6700 g.mol^{-1}), it was interesting to observe a substantial difference in N_{agg} (5.4×10^4 and 13.8×10^4, respectively) according to SLS data despite possessing similar D_h as indicated by DLS. This could be attributed to the difference in polydispersity between the two samples, or even possibly a difference in the packing arrangement of the different glycopolymers. Nonetheless, the narrow polydispersity indices (PDI ≤ 0.1), large hydrodynamic diameters (D_h > 200 nm) and aggregation numbers ($N_{agg} > 5 \times 10^4$) determined *via* DLS and SLS support the hypothesis that the self-assemblies were of vesicular morphology.

Table 2. Light scattering data for PDMS-glyco-polymersomes in water prepared *via* solvent switch.

Entry	$M_{n,th}$[a] (g.mol^{-1})	$D_{h\ (z\text{-}av)}$ (nm)	PDI	d*n*/d*c*[b] (mL.g^{-1})	M_{app} (g.mol^{-1})	N_{agg}
P1$_{Glu}$	6700	212	0.11	0.301	3.46×10^8	5.40×10^4
P1$_{Gal}$	6700	221	0.02	0.254	8.81×10^8	1.38×10^5
P2$_{Glu}$	9600	337[c]	0.46[c]	-	-	-

P2$_{Gal}$	9600	325	0.21	-	-	-

[a] Theoretical molar mass of block copolymers assuming quantitative substitution of precursor.

[c] d*n*/d*c* determined using a differential refractometer.

[c] Bimodal distribution: populations at 600 nm and 25 nm (see supporting information).

DLS conducted at 0.5 mg.ml^{-1}

Transmission electron microscopy (TEM) was performed to further assess the morphology of the self-assemblies of **P1$_{Glu}$** and **P1$_{Gal}$** (Fig. 2d and S13). Individual spherical objects are observed with diameters ranging from 150 and 250 nm, which is in good agreement with the DLS data obtained, and in the case of **P1$_{Glu}$** it is possible to discern a bilayer membrane (Fig. 2d). Interestingly, in some instances for the self-assemblies of **P1$_{Glu}$** multiple lamellae could be observed, which may indicate that some species were in fact multilamellar polymersomes, or possibly unilamellar polymersomes which had flattened into an ordered thin film (Fig. S13). In other cases, multilamellar objects which could potentially be explained by the "fusing" of two or more polymersomes may be observed (Fig. S13). The occurrence of these interesting formations could possibly be due to re-organization of the very flexible polymeric membrane during sample preparation for dry-state TEM.

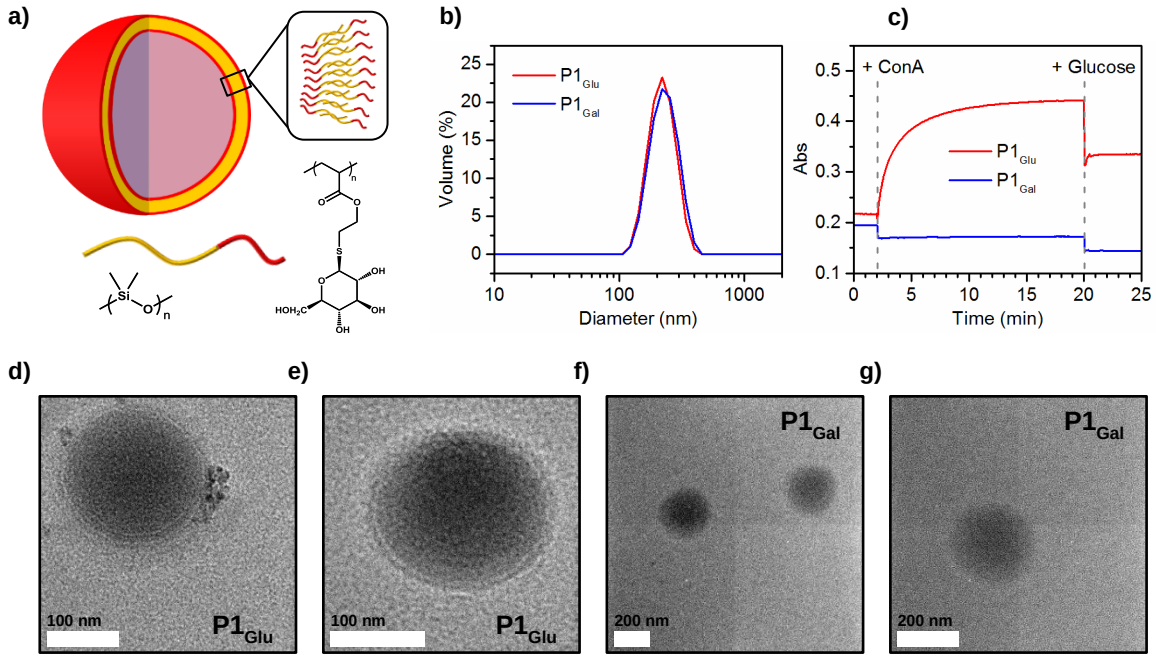

Figure 2. Schematic of self-assembled polymersomes **(a)**. DLS traces of **P1$_{Glu}$** (red trace) and **P1$_{Gal}$** (blue trace) polymersomes at 0.5 mg.mL^{-1} in phosphate buffer (pH 7) **(b)**. Absorbance profiles of **P1$_{Glu}$** (red trace) and **P1$_{Gal}$** (blue trace) polymersomes in phosphate buffer (pH 7) upon the addition of concanavalin A (2 mins) and concentrated glucose solution (20 mins) **(c)**. TEM micrographs of **P1$_{Glu}$** polymersomes (scale bar is 100 nm) **(d/e)**. TEM micrograph of **P1$_{Gal}$** polymersomes (scale bar is 200 nm) **(f/g)**.

Encouraged that the **P1$_{Glu}$** and **P1$_{Gal}$** diblock copolymer compositions were self-assembling to adopt the desired vesicular morphology, turbidimetric experiments were conducted with the glycosylated polymersomes to demonstrate the availability of carbohydrate moieties in solution and the selectivity of their binding behaviour with lectins. The lectin concanavalin A (Con A), which possesses a strong binding affinity for mannose and glucose, was chosen to demonstrate the selective binding of glucose-decorated polymersomes (**P1$_{Glu}$**).[67, 73-74] Addition of Con A to **P1$_{Glu}$** in PBS (pH 7, DLS traces prior to Con A addition shown in Fig. 2b) resulted in an increase in absorbance due to aggregation of the polymersomes, while for the galactose-decorated polymersomes (**P1$_{Gal}$**) only a small decrease in absorbance was observed due to dilution (Fig. 2c). The subsequent addition of excess glucose resulted in a sharp decrease in absorbance for **P1$_{Glu}$**, indicating partial breakdown of the aggregates, while again only a small decrease in absorption was observed for **P1$_{Gal}$** polymersomes due to dilution. The response of the **P1$_{Gal}$** polymersomes towards Con A and excess glucose respectively indicate a reversible, non-covalent binding mechanism characteristic of carbohydrate-lectin interactions.

Meanwhile, application of the same solvent-switch method with **P2$_{Glu}$** and **P2$_{Gal}$** resulted in the observation of poorly-defined populations, exhibiting large hydrodynamic volumes and broad size distributions (Table 2). Indeed, in the case of **P2$_{Glu}$** a bimodal distribution was observed with populations of substantially different diameter (≈ 600 nm and ≈ 25 nm) (Fig. S14).

Formation of giant glycosylated polymersomes (GGPs) and their interaction with *fim*H positive *E. coli*.

Having demonstrated that the novel PDMS-glycopolymers **P1$_{Glu}$** and **P1$_{Gal}$** could undergo self-assembly in solution to form vesicular morphologies and that the membranes of the polymersomes may undergo selective binding with lectins, attention turned towards generating GGPs as a simple synthetic cell mimic. As mentioned above, the average size and size distribution of polymersomes for a certain block copolymer composition is strongly dependent on the formation process.[20, 72] Micron-scale polymersomes have been reported previously using an electroformation process, a film-rehydration method whereby rehydration is induced under an oscillating electric field.[24, 75-76] For **P1$_{Glu}$** and **P1$_{Gal}$,** the electroformation method used was adapted from previous work by Kubilis *et al*.[53] A custom-made electroformation apparatus was employed in this study. Polymer solutions containing rhodamine B octadecyl ester perchlorate were deposited on the surfaces of both electrodes of indium tin oxide-coated glass plates in the electroformation apparatus. Application of AC voltage between the two electrodes during the swelling of the polymer film in water led to the formation of stable unilamellar GGPs with sizes ranging from approximately 2 - 20 μm in diameter as revealed by fluorescent laser scanning confocal microscopy (LSCM) (Fig. 3a/b and S15).

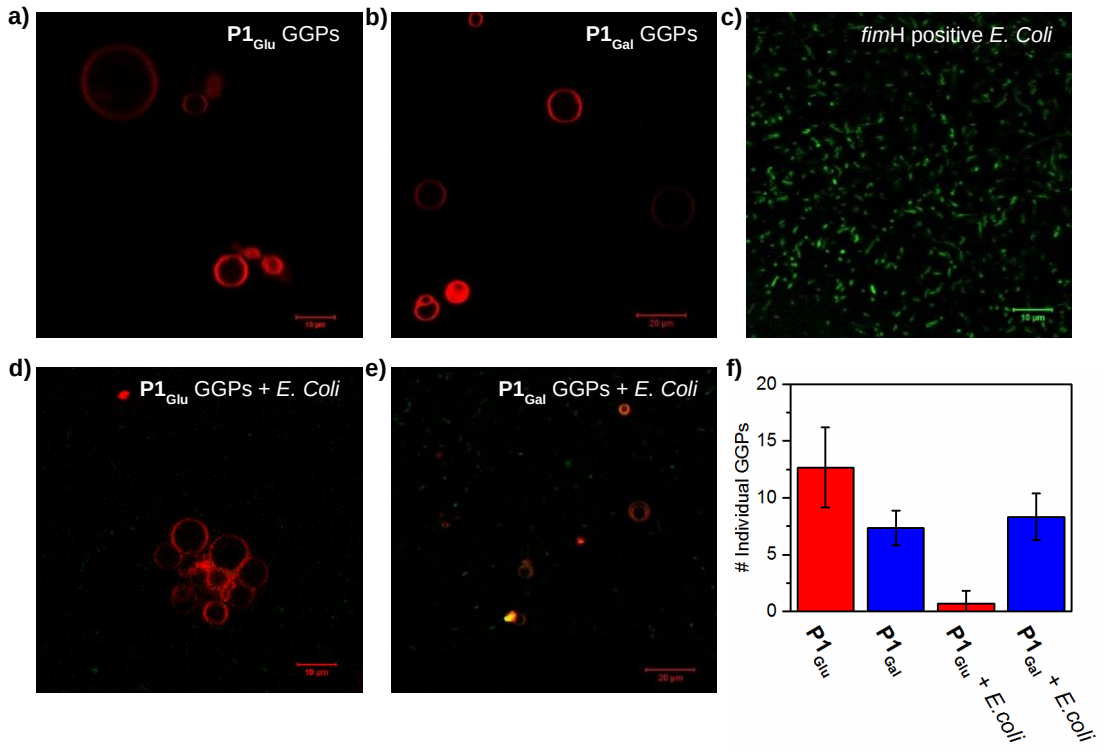

Figure 3. Giant glycosylated polymersomes of **P1$_{Glu}$** (Scale bar 10 μm) **(a)** and **P1$_{Gal}$** (Scale bar 20 μm) **(b)**. CFP-fluorescent *E. coli* (DH5α) (*fim*H positive) in PBS (Scale bar 10 μm) **(c)**. **P1$_{Glu}$** GGPs **(d)** and **P1$_{Gal}$** GGPs **(e)** following the addition of the (*fim*H positive) *E. coli* (Scale bars 10 and 20 μm respectively). The giant polymersome membranes were stained with rhodamine B octadecyl ester perchlorate during the electroformation process. Numbers of individual GGPs observed *via* confocal fluorescence microscopy before and after the addition of the (*fim*H positive) *E. coli* **(f)**.

The GGPs were then employed in interaction studies with a cyan fluorescent protein (CFP) fluorescent *E. coli* strain (DH5α) expressing the *fim*H protein, a bacterial adhesion which exhibits strong selectivity towards mannose (k_d = 2.3 μM).[77] Importantly, for the purpose of these interaction studies, *fim*H possesses greater binding affinity for glucose (k_d = 9.2 mM) than galactose (k_d = 100 mM), and therefore the different GGPs could be expected to interact differently in the presence of the bacteria.[77] Interestingly, the glucose-decorated GGPs **(P1$_{Glu}$)** were observed to form large clusters following addition of the *fim*H positive *E. coli*, believed to be driven by the carbohydrate-lectin interactions (Fig. 3d and S15). Indeed, almost no individual GGPs were observed (Fig. 3f). This clustering effect would suggest that the interactions between glucose-decorated GGPs and the bacteria are relatively strong by

virtue of the multivalent presentation of glucose moieties despite *fim*H only possessing moderate affinity towards this carbohydrate. Furthermore, it was interesting that individual GGPs within the clusters, while appearing slightly diminished in size compared to the GGPs without the presence of *E. coli*, maintained their vesicular morphology.

In contrast, the galactose-decorated GGPs **($P1_{Gal}$)** do not cause substantial clustering, and in most cases the GGPs were present individually (Fig. 2f). However, there was evidence that the GGPs and *fim*H positive *E. coli* were interacting (Fig. 2e and S15). It was interesting to observe strong colocalized fluorescence around the lamellar of the **$P1_{Gal}$** GGPs which was not observed with the **$P1_{Glu}$** GGPs. This would indicate that there is still some level of interaction between the galactose-decorated GGPs due to the large abundance of galactose moieties, although not strong enough to induce clustering as in the case of the glucose-decorated GGPs. That both GGPs are able to interact with the *E. coli* with profoundly difference outcomes due to the differing strength of the respective carbohydrate-lectin interactions, is an extremely interesting and exciting observation. The potential to modulate the response of these protocell models towards bacteria, either by instigating clustering of GGPs around the bacteria or simply immobilizing bacteria onto the surface of individual GGPs though selection of the appropriate carbohydrate moiety could be exploited for different biological applications.

Conclusion

A novel amphiphilic diblock copolymer composed of a highly flexible PDMS hydrophobic block and a biologically-relevant glycopolymer hydrophilic block was synthesized in this work. Using a PDMS macroCTA, well-defined PDMS-*b*-pBEA diblock copolymers were prepared *via* RAFT polymerization ($Đ$ = 1.1) which could then be substituted post-polymerization under facile conditions (room temperature) to yield the desired copolymer composition. Compositions possessing ≈ 25 % glycopolymer block (by mass) were able to adopt a vesicular morphology in solution, which was demonstrated on both the nanoscale and microscale by utilizing different self-assembly processes. The ability of these polymersomes to interact with biological receptors was also demonstrated on both the nanoscale and microscale, using ConA and *fim*H positive *E. coli* respectively. Excitingly, in the latter

system the differing strength in carbohydrate-lectin interactions between GGPs possessing different carbohydrates resulted in profoundly disparate responses. Using this approach, the hydrophilic/hydrophobic balance of the resulting diblock copolymer may be readily controlled through RAFT polymerization, while a number of different sugars may be introduced through a single precursor in a facile synthetic procedure. These features may enable both the morphology, and the biological interaction of subsequent self-assemblies to be readily tuned. To this end, we believe that the electroformed giant (cell-sized) glycosylated polymersomes represent a unique example of a synthetic system that displays a cellular behavior.

Funding Sources

Royal Society Wolfson Merit Award (WM130055; SP); Monash-Warwick Alliance (LM, JZ, AME, NRC, SP), Engineering and Physical Sciences Research Council (1499928; PG) and the German Research Foundation (DFG, GZ: HA 7725/1-1; MH).

Acknowledgements

We thank the Royal Society Wolfson Merit Award (WM130055; SP), the Monash-Warwick Alliance (LM, JZ, AME, NRC, SP), European Research Council (TUSUPO 647106; SP), Engineering and Physical Sciences Research Council (1499928; PG) and the German Research Foundation (DFG, GZ: HA 7725/1-1; MH). We are grateful for the Research Technology Platform (RTP) in Polymer Characterization at Warwick Chemistry for providing use of GPC/SEC and the RTP in Advanced Bioimaging at Warwick School of Life Sciences for providing access to microscopy suite. The authors thank Dr. Francisco Fernández-Trillo (University of Birmingham) and Prof. Anne-Marie Krachler (UTHealth, US) for the kind donation of *E. coli* strains.

Experimental Section

Materials

Acryloyl chloride, 2-bromoethanol, 4-(dimethylamino)pyridine, anhydrous dimethyl sulfoxide, methanol, anhydrous *N*-methyl-2-pyrrolidone, poly(dimethylsiloxane) (monohydroxy terminated, average M_n ~ 4,670 g.mol^{-1}) and 1-thio-*β*-D-glucose sodium salt, 4-(dimethylamino)pyridine (DMAP) and rhodamine B octadecyl ester perchlorate were obtained from Sigma-Aldrich. *D*-glucose anhydrous, dimethyl sulfoxide, 1,4-dioxane, tetrahydrofuran and triethylamine were obtained from Fisher Scientific. Chloroform and dichloromethane were obtained from VWR. Dimethyl 2,2'-azobis(2-methylpropionate) (V-601) was obtained from Wako Chemicals. *N*-(3-dimethylaminopropyl)-*N*'-ethylcarbodiimide hydrochloride (EDC.HCl) was obtained from Iris Biotech. 1-thio-*β*-D-galactose sodium salt was obtained from Carbosynth. Concanavalin A was obtained from MP biomedicals. Carbon coated TEM grids were obtained from EM Resolutions (UK). The chain transfer agent 2-(((butylthio)-carbonothioyl)thio)propanoic acid, called (propanoic acid)yl butyl trithiocarbonate (PABTC), was synthesized according to a previously reported protocol.[78] The CFP bacteria used are DH5α *E.coli* (non-pathogenic lab strain) transformed with the plasmid PSF-OXB20-FRCFP and were supplied by the lab of Dr Fernandez-Trillo at the University of Birmingham. This plasmid gives the bacteria resistance to Kanamycin at 50 μg.ml^{-1} final concentration. The bacteria were maintained on LB agar plates or grown in LB media liquid broth, both supplemented with Kanamycin and incubated at 37 °C overnight. LB Agar plates with bacteria are stored at 4 °C.

Methods

Nuclear Magnetic Resonance (NMR) spectroscopy: NMR spectra of the PDMS-PBTC and PDMS-*b*-PBEA block copolymers **P1** and **P2** (in $CDCl_3$) were recorded on a Bruker Avance III 400 HD MHz spectrometer at 25 °C (298 K):^{1}H (400 MHz), ^{13}C (100 MHz). HSQC and associated ^{1}H NMR spectra of PDMS-*b*-pBEA **P1** and **P2**, PDMS-*b*-2(2-(1-*β*-D-thioglucose)ethyl acrylate) $\mathbf{P1_{Glu}}$ and $\mathbf{P2_{Glu}}$, and PDMS-*b*-P(2-(1-*β*-D-thiogalactose)ethyl acrylate) $\mathbf{P1_{Gal}}$ and $\mathbf{P2_{Gal}}$ (in THF-d_8/Methanol-d_4) were recorded using a Bruker Avance III 500 MHz spectrometer at 25 °C (298 K): ^{1}H (500 MHz), ^{13}C (125 MHz).

Size Exclusion Chromatography (SEC): SEC was conducted using an Agilent 390-LC MDS instrument equipped with differential refractive index (DRI) and dual wavelength UV detectors. The system was equipped with a PLgel 5 μm guard column followed by 2 x PLgel Mixed C columns (300 x 7.5 mm). The eluent was THF with 2 % TEA (triethylamine) and 0.01 % BHT (butylated hydroxytoluene) additives. Samples were run at 1 ml/min at 30 °C. Poly(methyl methacrylate) (Agilent EasyVials) narrow standards with a molar mass range of 5.5×10^2 to 1.568×10^6 g.mol^{-1} were used to calibrate the SEC system. Analyte samples were filtered through a polytetrafluoroethylene (PTFE) membrane with 0.2 μm pore size prior to injection. Experimental molar mass ($M_{n,SEC}$) and dispersity ($Đ$) values of the synthesised polymers were determined using Agilent GPC/SEC software.

Differential Scanning Calorimetry (DSC): Thermal transitions of PDMS-containing diblock polymers were measured under nitrogen on a Mettler Toledo DSC1. Three heating and cooling cycles in a temperature range of -123.15 K (-150 °C) to 453.15 K (180 °C) were performed at a scan rate of 10 K.min^{-1}.

Dynamic Light Scattering (DLS): Size measurements were conducted on a Malvern Zetasizer Nano-ZS at 25 °C with a 4 mW He-Ne 633 nm laser at a scattering angle of 173 ° (back scattering), assuming the refractive of PDMS (1.410). The measurements were repeated three times with automatic attenuation selection and measurement position. Results were analyzed using Malvern DTS 6.20 software.

Static light scattering (SLS): Light scattering measurements were conducted using an ALV-CGS3 system operating with a vertically polarized laser with the wavelength λ = 632 nm. Measurements were taken at 25 °C over a range of scattering wave vectors ($q = 4\pi n\sin(\theta/2)/\lambda$, where θ is the angle of observation and n the refractive index of the solvent. The incremental refractive indices (dn/dC) of $\mathbf{P1_{Glu}}$ and $\mathbf{P1_{Gal}}$ solutions were determined by measuring their refractive indices at concentrations ranging from 0.1 to 0.01 mg.mL^{-1} using a Shodex RI detector operating at a wavelength of 632 nm.

Transmission electron microscopy (TEM): The carbon-coated TEM grids were glow discharged prior to sample preparation to increase the hydrophilicity of the surface. For sample preparation, 10 μL of a 0.2 mg.mL^{-1} solution of polymer self-assemblies in water was placed onto the TEM grid and left for 60

seconds. The grid was then blotted dry with filter paper. Images were obtained on a JEOL2011 200 kV LaB6 transmission electron microscope fitted with a Gatan Ultrascan™ 1000 camera.

Confocal fluorescence microscopy: Confocal fluorescence microscopy images were taken with a Zeiss 880 LSM with sequential argon laser imaging using wavelengths of 488 nm (CFP) and 514 nm (Rhodamine B octadecyl ester perchlorate). Unless stated otherwise, laser intensity was set to 5 %, with pinhole diameter at 76.1 μm. Images were taken with 40 and 63x oil immersion lenses.

UV/Vis turbidity experiments: Absorbance measurements were conducted using an Agilent Carey 60 UV-Vis spectrometer. For turbidimetric studies, a 0.5 mg/mL solution of $\mathbf{P1_{Glu}}$ vesicles were prepared by dilution of a 2.0 mg/mL aqueous solution with water (to 1 $mg.mL^{-1}$) followed by phosphate buffer (0.05 $mol.L^{-1}$) to give a final concentration of 0.5 $mg.mL^{-1}$ (in 0.025 $mol.L^{-1}$ PB buffer). For measurements 0.8 mL of this solution was transferred to a 4.5 mL polystyrene cuvette, and absorbance readings were collected every second at 500 nm. After 2 minutes, 0.2 mL of a 2.0 $mg.mL^{-1}$ solution of concanavalin A in PB ($\approx 2 \times 10^{-5}$ $mol.L^{-1}$) was introduced and quickly mixed using an Eppendorf pipette. After another 18 minutes, 0.2 mL of a 100 $mg.mL^{-1}$ D-glucose solution was introduced and quickly mixed using an Eppendorf pipette. Readings were collected using Agilent Carey WinUV kinetics application software.

GGP interactions with *E. coli*: A single colony was suspended in phosphate-buffered saline (PBS; pH 7.4, 100 μL). With a micropipette, an aliquot of 50 μL was added slowly to the GGPs in ultrapure water and incubated for 30 min to allow stabilization of GGPs before imaging using fluorescence confocal microscopy.

Synthesis

Synthesis of 2-bromoethyl acrylate (BEA): BEA monomer was synthesized according to a previously reported procedure.[66, 79] In a typical reaction, 2-bromoethanol (67 g, 38 mL, 0.54 mol) was dissolved in CH_2Cl_2 (300 mL), to which triethylamine (82.2 mL, 59.7 g, 0.59 mol) was added under a nitrogen atmosphere, and the reaction was cooled to 0 °C. Acryloyl chloride (47.9 g, 53.4 mL, mol) in CH_2Cl_2 (30 mL) was subsequently added dropwise over an hour with stirring. The reaction was allowed to warm

to room temperature overnight with continued stirring. Upon completion, the reaction mixture was filtered, the solid residue washed with CH_2Cl_2, and the organic layer washed with water (2 × 100 mL) and then brine (2 × 100 mL). The organic layer was dried over anhydrous $MgSO_4$ and filtered, and the solvent was removed under reduced pressure. The product was purified by distillation under reduced pressure (~1 mbar, 39−40 °C) to give 2-bromoethyl acrylate as a clear colorless liquid in 80 % yield; bp 41−43 °C (0.68 mmHg). ^{1}H NMR (400 MHz, 298 K, $CDCl_3$, δ): 6.42 (dd, J = 17.4, 1.3 Hz, 1 H, −C=CH_2), 5.82 (dd, J = 17.4, 10.5 Hz, 1 H, CH_2=CH−), 6.08 (dd, J = 10.5, 1.3 Hz, 1 H, −C=CH_2), 4.40 (t, J = 6.1 Hz, 2 H, −O−CH_2−CH_2−), 3.48 (t, J = 6.2 Hz, 2 H, −CH_2−CH_2−Br).

Synthesis of PDMS-PBTC: The PDMS-PBTC macro-CTA was prepared *via* an EDCI/DMAP-catalyzed esterification of the carboxylic acid R group of the PABTC CTA with the ω-chain end hydroxyl of the PDMS according to a previously reported procedure.[60] A solution of *N*-(3-dimethylaminopropyl)-*N*'-ethylcarbodiimide hydrochloride (EDCI) (0.754 g, 3.93 mmol) in dichloromethane (25 mL) was added drop-wise to a solution of PDMS-OH (13.1 g, 2.81 mmol), PABTC (1.000 g, 4.19 mmol) and DMAP (0.051 g, 0.42 mmol) in dichloromethane (10 mL) at < 10 °C. Following addition, the reaction was allowed to stir for 16 hours at room temperature. The opaque red/orange solution was washed with 1 M sodium hydroxide solution (2 x 60 mL) and distilled water (2 x 60 mL). The organic layer was dried over $MgSO_4$, concentrated under vacuum and purified by flash chromatography (silica, 100 % dichloromethane). The purified macro-CTA was concentrated under vacuum to afford the product as yellow oil (yield: 8.931 g, 65 %). ^{1}H NMR (400 MHz, 298 K, $CDCl_3$, δ:) 4.29 (2H, t, J = 5.6 Hz, O–CH_2–CH_2–CO_2), 3.69 (2H, t, O–CH_2–CH_2–CO_2), 4.84 (1H, q, J = 7.3 Hz, S–CH(CH_3)–CO_2), 3.42 (2H, t, J = 7.0 Hz, O–CH_2–$(CH_2)_2$–Si), 3.35 (2H, t, J = 7.4 Hz, CH_2–CH_2–S), 0.93 (3H, t, J = 7.3 Hz, CH_3–$(CH_2)_3$–S), 0.89 (3H, t, J = 7.1 Hz, CH_3–$(CH_2)_3$–Si), 1.43 (2H, m, CH_3–CH_2– CH_2–CH_2–S), 1.64–1.71 (4H, m, CH_3–$(CH_2)_3$–Si, 1.61–1.63 (3H, d, J = 7.4 Hz, S–CH(CH_3)–CO_2), 0.07 (3H, m, Si(CH_3)$_2$–O).

Synthesis of PDMS-pBEA diblock copolymers: $PDMS_{60}$-PBTC (0.898 g, 0.926 mL, 0.184 mmol), BEA (0.327 g, 0.226 mL, 1.837 mmol), 1,4-dioxane (2.065 g, 1.999 mL) and V-601 (10 mg.mL^{-1} solution in 1,4-dioxane, 0.194 g, 0.188 mL, 8.15 × 10^{-3} mmol) were added to a vial equipped with a

magnetic stirrer bar. The solution was bubbled with nitrogen for 15 minutes then placed into a thermostated oil bath set at 66 °C and allowed to stir for 4 h. The polymerization was stopped by cooling the reaction to room temperature and exposure to air. The crude polymer was precipitated directly into MeOH/H_2O (70:30), re-dissolved in THF (≈ 3 mL) and precipitated again into MeOH/H_2O. The precipitated polymer was dissolved in THF (≈ 3 mL) and the solvent removed under reduced pressure to yield $PDMS_{60}$-*b*-$PBEA_6$ as a yellow oil (1.010 g). The degree of polymerization (DP_n) of purified PDMS-PBEA polymers were determined by comparing the integrals of the peak(s) from 0.4 – 0.5 ppm (4 protons, assigned d and f in fig. 1) with the peaks from 3.4 – 3.6 ppm (assigned z and i in **Fig. 1**):

Post-polymerization substitution with 1-thio-*β*-D-glucose: $PDMS_{60}$-*b*-$PBEA_6$ **(P1)** (0.228 g, 0.038 mmol, 0.229 mmol BEA moieties) was added to a 20 mL vial equipped with a magnetic stirrer bar. The vial was sealed with a rubber septum and purged with nitrogen. Anhydrous NMP (5.20 mL) and anhydrous DMSO (2.80 mL) were introduced *via* syringe and the polymer was allowed to dissolve resulting in a turbid yellow solution. Nitrogen was bubbled through the solution for 20 mins. 1-thio-*β*-D-glucose sodium salt (0.101 g, 0.458 mmol in 5.10 mL anhydrous DMSO) was introduced *via* syringe (final DMSO:NMP ratio of 60:40, by volume). Nitrogen was bubbled through the solution for 20 and the substitution was left stirring under nitrogen for 16 h at room temperature. The resulting clear yellow solution was diluted with distilled water and dialyzed against distilled water (MWCO: 1 kDa). The volume of water was reduced and $PDMS_{60}$-*b*-P(2-(1-thio-*β*-D-glucose)ethyl acrylate)$_6$ **($P1_{Glu}$)** was obtained as a white solid following lyophilization. Substitution of $PDMS_{60}$-*b*-$PBEA_{16}$ **(P2)** was performed in the same manner with the final DMSO:NMP ratio set at 65:35 (by volume) to yield **$P2_{Glu}$.**

Post-polymerization substitution with 1-thio-*β*-D-galactose: $PDMS_{60}$-*b*-$PBEA_6$ **(P1)** (0.226 g, 0.038 mmol, 0.228 mmol BEA moieties) was added to a 50 mL round-bottomed flask equipped with a magnetic stirrer bar. Anhydrous NMP (9.00 mL) and anhydrous DMSO (3.60 mL) were introduced *via* syringe and the polymer was allowed to dissolve resulting in a yellow solution. Nitrogen was bubbled through the solution for 20 mins. 1-thio-*β*-D-galactose sodium salt (0.104 g 0.456 mmol, dissolved in 10.40 mL DMSO and 0.80 mL distilled water) was introduced *via* syringe (final DMSO:NMP:H_2O ratio of 59:38:3, by volume). Nitrogen was bubbled through the solution for 20 and the substitution was

left stirring under nitrogen for 16 h at room temperature. The resulting clear yellow solution was diluted with distilled water and dialyzed against distilled water (MWCO: 1 kDa). The volume of water was reduced and $PDMS_{60}$-*b*-P(2-(1-thio-*β*-D-galactose)ethyl acrylate)$_6$ **($P1_{Gal}$)** was obtained as a white solid following lyophilization. Substitution of the $PDMS_{60}$-*b*-$PBEA_{16}$ **(P2)** was performed in the same manner with the final DMSO:NMP:H_2O ratio set at 63:34:3 (by volume) to yield **$P2_{Gal}$**.

Self-assembly of PDMS-glycopolymers *via* solvent switch: A fresh solution of block copolymer (3.81 $mg.mL^{-1}$) in THF/MeOH (95/5 *v*/*v*) was prepared in a glass vial equipped with a magnetic stirrer bar. Distilled water was added gradually with gentle stirring to give a final polymer concentration of 2 $mg.mL^{-1}$ following removal of the organic solvents. The solutions were allowed to stir for two days to allow the organic solvents to evaporate.

Self-assembly of PDMS-glycopolymers *via* Electroformation process: Giant polymersomes of **$P1_{Glu}$** and **$P1_{Gal}$** were prepared using a previously reported electroformation procedure and setup.[53] A 20 μL solution of **$P1_{Glu}$** in THF/MeOH (3:1 *v*/*v*) (5 $mg.mL^{-1}$), containing rhodamine B octadecyl ester perchlorate (0.05 wt. %) was deposited on two indium tin oxide (ITO) coated glass slide electrodes. The solvent was removed under reduced pressure to form thin films on the ITO slides. A rubber spacer filled with MilliQ water (250 μL) was sandwiched between the two slide electrodes. An electric field (1.2 V, 10 Hz, sinusoidal wave form) was applied for 18 h to yield giant polymersomes. The resulting giant polymersome-containing solution was transferred to a glass slip bottomed container.

References

1. Fishkis, M., Steps Towards the Formation of A Protocell: The Possible Role of Short Peptides. *Origins of Life and Evolution of Biospheres* **2007,** *37* (6), 537-553.

2. LeDuc, P. R.; Wong, M. S.; Ferreira, P. M.; Groff, R. E.; Haslinger, K.; Koonce, M. P.; Lee, W. Y.; Love, J. C.; McCammon, J. A.; Monteiro-Riviere, N. A.; Rotello, V. M.; Rubloff, G. W.; Westervelt, R.; Yoda, M., Towards an in vivo biologically inspired nanofactory. *Nat Nano* **2007,** *2* (1), 3-7.

3. Li, M.; Huang, X.; Tang, T. Y. D.; Mann, S., Synthetic cellularity based on non-lipid micro-compartments and protocell models. *Current Opinion in Chemical Biology* **2014,** *22*, 1-11.

4. Xu, C.; Hu, S.; Chen, X., Artificial cells: from basic science to applications. *Materials Today* **2016,** *19* (9), 516-532.

5. Buddingh', B. C.; van Hest, J. C. M., Artificial Cells: Synthetic Compartments with Life-like Functionality and Adaptivity. *Accounts of Chemical Research* **2017,** *50* (4), 769-777.

6. Tu, Y.; Peng, F.; Adawy, A.; Men, Y.; Abdelmohsen, L. K. E. A.; Wilson, D. A., Mimicking the Cell: Bio-Inspired Functions of Supramolecular Assemblies. *Chemical Reviews* **2016,** *116* (4), 2023-2078.

7. Meeuwissen, S. A.; Rioz-Martinez, A.; de Gonzalo, G.; Fraaije, M. W.; Gotor, V.; van Hest, J. C. M., Cofactor regeneration in polymersome nanoreactors: enzymatically catalysed Baeyer-Villiger reactions. *Journal of Materials Chemistry* **2011,** *21* (47), 18923-18926.

8. Jewett, M. C.; Swartz, J. R., Mimicking the Escherichia coli cytoplasmic environment activates long-lived and efficient cell-free protein synthesis. *Biotechnology and Bioengineering* **2004,** *86* (1), 19-26.

9. Hardy, M. D.; Yang, J.; Selimkhanov, J.; Cole, C. M.; Tsimring, L. S.; Devaraj, N. K., Self-reproducing catalyst drives repeated phospholipid synthesis and membrane growth. *Proceedings of the National Academy of Sciences* **2015,** *112* (27), 8187-8192.

10. Engelhart, A. E.; Adamala, K. P.; Szostak, J. W., A simple physical mechanism enables homeostasis in primitive cells. *Nat Chem* **2016,** *8* (5), 448-453.

11. Zhu, T. F.; Szostak, J. W., Coupled Growth and Division of Model Protocell Membranes. *Journal of the American Chemical Society* **2009,** *131* (15), 5705-5713.

12. Mansy, S. S.; Schrum, J. P.; Krishnamurthy, M.; Tobe, S.; Treco, D. A.; Szostak, J. W., Template-directed synthesis of a genetic polymer in a model protocell. *Nature* **2008,** *454* (7200), 122-125.

13. Dzieciol, A. J.; Mann, S., Designs for life: protocell models in the laboratory. *Chemical Society Reviews* **2012,** *41* (1), 79-85.

14. Walde, P.; Ichikawa, S., Enzymes inside lipid vesicles: preparation, reactivity and applications. *Biomolecular Engineering* **2001,** *18* (4), 143-177.

15. Noireaux, V.; Libchaber, A., A vesicle bioreactor as a step toward an artificial cell assembly. *Proceedings of the National Academy of Sciences of the United States of America* **2004,** *101* (51), 17669-17674.

16. Ishikawa, K.; Sato, K.; Shima, Y.; Urabe, I.; Yomo, T., Expression of a cascading genetic network within liposomes. *FEBS Letters* **2004,** *576* (3), 387-390.

17. Kurihara, K.; Tamura, M.; Shohda, K.-i.; Toyota, T.; Suzuki, K.; Sugawara, T., Self-reproduction of supramolecular giant vesicles combined with the amplification of encapsulated DNA. *Nat Chem* **2011,** *3* (10), 775-781.

18. Huang, X.; Li, M.; Green, D. C.; Williams, D. S.; Patil, A. J.; Mann, S., Interfacial assembly of protein–polymer nano-conjugates into stimulus-responsive biomimetic protocells. **2013,** *4*, 2239.

19. Priftis, D.; Laugel, N.; Tirrell, M., Thermodynamic Characterization of Polypeptide Complex Coacervation. *Langmuir* **2012,** *28* (45), 15947-15957.

20. LoPresti, C.; Lomas, H.; Massignani, M.; Smart, T.; Battaglia, G., Polymersomes: nature inspired nanometer sized compartments. *Journal of Materials Chemistry* **2009,** *19* (22), 3576-3590.

21. Howse, J. R.; Jones, R. A. L.; Battaglia, G.; Ducker, R. E.; Leggett, G. J.; Ryan, A. J., Templated formation of giant polymer vesicles with controlled size distributions. *Nat Mater* **2009,** *8* (6), 507-511.

22. Kita-Tokarczyk, K.; Grumelard, J.; Haefele, T.; Meier, W., Block copolymer vesicles—using concepts from polymer chemistry to mimic biomembranes. *Polymer* **2005,** *46* (11), 3540-3563.

23. Le Meins, J.-F.; Sandre, O.; Lecommandoux, S., Recent trends in the tuning of polymersomes' membrane properties. *The European Physical Journal E* **2011,** *34* (2), 14.

24. Discher, B. M.; Won, Y.-Y.; Ege, D. S.; Lee, J. C.-M.; Bates, F. S.; Discher, D. E.; Hammer, D. A., Polymersomes: Tough Vesicles Made from Diblock Copolymers. *Science* **1999,** *284* (5417), 1143-1146.

25. Bermudez, H.; Brannan, A. K.; Hammer, D. A.; Bates, F. S.; Discher, D. E., Molecular Weight Dependence of Polymersome Membrane Structure, Elasticity, and Stability. *Macromolecules* **2002,** *35* (21), 8203-8208.

26. Bermúdez, H.; Hammer, D. A.; Discher, D. E., Effect of Bilayer Thickness on Membrane Bending Rigidity. *Langmuir* **2004,** *20* (3), 540-543.

27. Jaskiewicz, K.; Makowski, M.; Kappl, M.; Landfester, K.; Kroeger, A., Mechanical Properties of Poly(dimethylsiloxane)-block-poly(2-methyloxazoline) Polymersomes Probed by Atomic Force Microscopy. *Langmuir* **2012,** *28* (34), 12629-12636.

28. Meier, W.; Nardin, C.; Winterhalter, M., Reconstitution of Channel Proteins in (Polymerized) ABA Triblock Copolymer Membranes. *Angewandte Chemie International Edition* **2000,** *39* (24), 4599-4602.

29. Nardin, C.; Widmer, J.; Winterhalter, M.; Meier, W., Amphiphilic block copolymer nanocontainers as bioreactors. *The European Physical Journal E* **2001,** *4* (4), 403-410.

30. Graff, A.; Sauer, M.; Van Gelder, P.; Meier, W., Virus-assisted loading of polymer nanocontainer. *Proceedings of the National Academy of Sciences* **2002,** *99* (8), 5064-5068.

31. Broz, P.; Driamov, S.; Ziegler, J.; Ben-Haim, N.; Marsch, S.; Meier, W.; Hunziker, P., Toward Intelligent Nanosize Bioreactors: A pH-Switchable, Channel-Equipped, Functional Polymer Nanocontainer. *Nano Letters* **2006,** *6* (10), 2349-2353.

32. Kumar, M.; Habel, J. E. O.; Shen, Y.-x.; Meier, W. P.; Walz, T., High-Density Reconstitution of Functional Water Channels into Vesicular and Planar Block Copolymer Membranes. *Journal of the American Chemical Society* **2012,** *134* (45), 18631-18637.

33. Gunkel-Grabole, G.; Sigg, S.; Lomora, M.; Lorcher, S.; Palivan, C. G.; Meier, W. P., Polymeric 3D nano-architectures for transport and delivery of therapeutically relevant biomacromolecules. *Biomaterials Science* **2015,** *3* (1), 25-40.

34. Lomora, M.; Garni, M.; Itel, F.; Tanner, P.; Spulber, M.; Palivan, C. G., Polymersomes with engineered ion selective permeability as stimuli-responsive nanocompartments with preserved architecture. *Biomaterials* **2015,** *53*, 406-414.

35. Lentini, R.; Yeh Martín, N.; Mansy, S. S., Communicating artificial cells. *Current Opinion in Chemical Biology* **2016,** *34*, 53-61.

36. Qiao, Y.; Li, M.; Booth, R.; Mann, S., Predatory behaviour in synthetic protocell communities. *Nat Chem* **2017,** *9* (2), 110-119.

37. Rudd, A. K.; Valls Cuevas, J. M.; Devaraj, N. K., SNAP-Tag-Reactive Lipid Anchors Enable Targeted and Spatiotemporally Controlled Localization of Proteins to Phospholipid Membranes. *Journal of the American Chemical Society* **2015,** *137* (15), 4884-4887.

38. Peters, R. J. R. W.; Nijemeisland, M.; van Hest, J. C. M., Reversibly Triggered Protein–Ligand Assemblies in Giant Vesicles. *Angewandte Chemie International Edition* **2015,** *54* (33), 9614-9617.

39. Sharon, N.; Lis, H., Lectins as cell recognition molecules. *Science* **1989,** *246* (4927), 227-234.

40. Dwek, R. A., Glycobiology: Toward Understanding the Function of Sugars. *Chemical Reviews* **1996,** *96* (2), 683-720.

41. Baenziger, J. U.; Fiete, D., Galactose and N-acetylgalactosamine-specific endocytosis of glycopeptides by isolated rat hepatocytes. *Cell* **1980,** *22* (2 Pt 2), 611-20.

42. Babiuch, K.; Dag, A.; Zhao, J.; Lu, H.; Stenzel, M. H., Carbohydrate-Specific Uptake of Fucosylated Polymeric Micelles by Different Cancer Cell Lines. *Biomacromolecules* **2015,** *16* (7), 1948-1957.

43. Kang, B.; Opatz, T.; Landfester, K.; Wurm, F. R., Carbohydrate nanocarriers in biomedical applications: functionalization and construction. *Chemical Society Reviews* **2015,** *44* (22), 8301-8325.

44. Srinivasarao, M.; Galliford, C. V.; Low, P. S., Principles in the design of ligand-targeted cancer therapeutics and imaging agents. *Nat Rev Drug Discov* **2015,** *14* (3), 203-219.

45. Liu, K.; Jiang, X.; Hunziker, P., Carbohydrate-based amphiphilic nano delivery systems for cancer therapy. *Nanoscale* **2016,** *8* (36), 16091-16156.

46. Li, X.; Chen, G., Glycopolymer-based nanoparticles: synthesis and application. *Polymer Chemistry* **2015,** *6* (9), 1417-1430.

47. Gauthier, M. A.; Gibson, M. I.; Klok, H.-A., Synthesis of Functional Polymers by Post-Polymerization Modification. *Angewandte Chemie International Edition* **2009,** *48* (1), 48-58.

48. von der Ehe, C.; Buś, T.; Weber, C.; Stumpf, S.; Bellstedt, P.; Hartlieb, M.; Schubert, U. S.; Gottschaldt, M., Glycopolymer-Functionalized Cryogels as Catch and Release Devices for the Pre-Enrichment of Pathogens. *ACS Macro Letters* **2016,** *5* (3), 326-331.

49. Das, S.; Sharma, D. K.; Chakrabarty, S.; Chowdhury, A.; Sen Gupta, S., Bioactive Polymersomes Self-Assembled from Amphiphilic PPO-GlycoPolypeptides: Synthesis, Characterization, and Dual-Dye Encapsulation. *Langmuir* **2015,** *31* (11), 3402-3412.

50. Gauche, C.; Lecommandoux, S., Versatile design of amphiphilic glycopolypeptides nanoparticles for lectin recognition. *Polymer* **2016,** *107*, 474-484.

51. Dai, X.-H.; Dong, C.-M., Synthesis, self-assembly and recognition properties of biomimetic star-shaped poly(ε-caprolactone)-b-glycopolymer block copolymers. *Journal of Polymer Science Part A: Polymer Chemistry* **2008,** *46* (3), 817-829.

52. Pasparakis, G.; Alexander, C., Sweet Talking Double Hydrophilic Block Copolymer Vesicles. *Angewandte Chemie International Edition* **2008,** *47* (26), 4847-4850.

53. Kubilis, A.; Abdulkarim, A.; Eissa, A. M.; Cameron, N. R., Giant Polymersome Protocells Dock with Virus Particle Mimics via Multivalent Glycan-Lectin Interactions. *Scientific Reports* **2016,** *6*, 32414.

54. Eissa, A. M.; Abdulkarim, A.; Sharples, G. J.; Cameron, N. R., Glycosylated Nanoparticles as Efficient Antimicrobial Delivery Agents. *Biomacromolecules* **2016,** *17* (8), 2672-2679.

55. Delorme, N.; Fery, A., Direct method to study membrane rigidity of small vesicles based on atomic force microscope force spectroscopy. *Physical Review E* **2006,** *74* (3), 030901.

56. Chen, Q.; Schönherr, H.; Vancso, G. J., Mechanical properties of block copolymer vesicle membranes by atomic force microscopy. *Soft Matter* **2009,** *5* (24), 4944-4950.

57. Perrier, S.; Takolpuckdee, P., Macromolecular design via reversible addition–fragmentation chain transfer (RAFT)/xanthates (MADIX) polymerization. *Journal of Polymer Science Part A: Polymer Chemistry* **2005,** *43* (22), 5347-5393.

58. Moad, G.; Rizzardo, E.; Thang, S. H., Living Radical Polymerization by the RAFT Process A Second Update. *Australian Journal of Chemistry* **2009,** *62* (11), 1402-1472.

59. Moad, G.; Rizzardo, E.; Thang, S. H., Living Radical Polymerization by the RAFT Process – A Third Update. *Australian Journal of Chemistry* **2012,** *65* (8), 985-1076.

60. Zhao, W.; Fonsny, P.; FitzGerald, P.; Warr, G. G.; Perrier, S., Unexpected behavior of polydimethylsiloxane/poly(2-(dimethylamino)ethyl acrylate) (charged) amphiphilic block copolymers in aqueous solution. *Polymer Chemistry* **2013,** *4* (6), 2140-2150.

61. Lopez-Oliva, A. P.; Warren, N. J.; Rajkumar, A.; Mykhaylyk, O. O.; Derry, M. J.; Doncom, K. E. B.; Rymaruk, M. J.; Armes, S. P., Polydimethylsiloxane-Based Diblock Copolymer Nano-objects Prepared in Nonpolar Media via RAFT-Mediated Polymerization-Induced Self-Assembly. *Macromolecules* **2015,** *48* (11), 3547-3555.

62. Pavlović, D.; Linhardt, J. G.; Künzler, J. F.; Shipp, D. A., Synthesis and Characterization of PDMS-, PVP-, and PS-Containing ABCBA Pentablock Copolymers. *Macromolecular Chemistry and Physics* **2010,** *211* (13), 1482-1487.

63. Pavlović, D.; Linhardt, J. G.; Künzler, J. F.; Shipp, D. A., Synthesis of amphiphilic multiblock and triblock copolymers of polydimethylsiloxane and poly(N,N-dimethylacrylamide). *Journal of Polymer Science Part A: Polymer Chemistry* **2008,** *46* (21), 7033-7048.

64. Karunakaran, R.; Kennedy, J. P., Novel amphiphilic conetworks by synthesis and crosslinking of allyl-telechelic block copolymers. *Journal of Polymer Science Part A: Polymer Chemistry* **2008,** *46* (12), 4254-4257.

65. Slavin, S.; Burns, J.; Haddleton, D. M.; Becer, C. R., Synthesis of glycopolymers via click reactions. *European Polymer Journal* **2011,** *47* (4), 435-446.

66. Barlow, T. R.; Brendel, J. C.; Perrier, S., Poly(bromoethyl acrylate): A Reactive Precursor for the Synthesis of Functional RAFT Materials. *Macromolecules* **2016,** *49* (17), 6203-6212.

67. Pröhl, M.; Englert, C.; Gottschaldt, M.; Brendel, J. C.; Schubert, U. S., RAFT polymerization and thio-bromo substitution: An efficient way towards well-defined glycopolymers. *Journal of Polymer Science Part A: Polymer Chemistry* **2017,** *55* (21), 3617-3626.

68. Blanazs, A.; Armes, S. P.; Ryan, A. J., Self-Assembled Block Copolymer Aggregates: From Micelles to Vesicles and their Biological Applications. *Macromolecular Rapid Communications* **2009,** *30* (4-5), 267-277.

69. Du, J.; O'Reilly, R. K., Advances and challenges in smart and functional polymer vesicles. *Soft Matter* **2009,** *5* (19), 3544-3561.

70. Mai, Y.; Eisenberg, A., Self-assembly of block copolymers. *Chemical Society Reviews* **2012,** *41* (18), 5969-5985.

71. Brinkhuis, R. P.; Rutjes, F. P. J. T.; van Hest, J. C. M., Polymeric vesicles in biomedical applications. *Polymer Chemistry* **2011,** *2* (7), 1449-1462.

72. Bleul, R.; Thiermann, R.; Maskos, M., Techniques To Control Polymersome Size. *Macromolecules* **2015,** *48* (20), 7396-7409.

73. Cairo, C. W.; Gestwicki, J. E.; Kanai, M.; Kiessling, L. L., Control of Multivalent Interactions by Binding Epitope Density. *Journal of the American Chemical Society* **2002,** *124* (8), 1615-1619.

74. Gurnani, P.; Lunn, A. M.; Perrier, S., Synthesis of mannosylated and PEGylated nanoparticles via RAFT emulsion polymerisation, and investigation of particle-lectin aggregation using turbidimetric and DLS techniques. *Polymer* **2016,** *106*, 229-237.

75. Lee, J. C. M.; Bermudez, H.; Discher, B. M.; Sheehan, M. A.; Won, Y.-Y.; Bates, F. S.; Discher, D. E., Preparation, stability, and in vitro performance of vesicles made with diblock copolymers. *Biotechnology and Bioengineering* **2001,** *73* (2), 135-145.

76. Dimova, R.; Seifert, U.; Pouligny, B.; Förster, S.; Döbereiner, H.-G., Hyperviscous diblock copolymer vesicles. *The European Physical Journal E* **2002,** *7* (3), 241-250.

77. Bouckaert, J.; Berglund, J.; Schembri, M.; De Genst, E.; Cools, L.; Wuhrer, M.; Hung, C.-S.; Pinkner, J.; Slättegård, R.; Zavialov, A.; Choudhury, D.; Langermann, S.; Hultgren, S. J.; Wyns, L.; Klemm, P.; Oscarson, S.; Knight, S. D.; De Greve, H., Receptor binding studies disclose a novel class of high-affinity inhibitors of the Escherichia coli FimH adhesin. *Molecular Microbiology* **2005,** *55* (2), 441-455.

78. Ferguson, C. J.; Hughes, R. J.; Nguyen, D.; Pham, B. T. T.; Gilbert, R. G.; Serelis, A. K.; Such, C. H.; Hawkett, B. S., Ab Initio Emulsion Polymerization by RAFT-Controlled Self-Assembly. *Macromolecules* **2005,** *38* (6), 2191-2204.

79. Choi, J.-H.; Ye, Y.; Elabd, Y. A.; Winey, K. I., Network Structure and Strong Microphase Separation for High Ion Conductivity in Polymerized Ionic Liquid Block Copolymers. *Macromolecules* **2013,** *46* (13), 5290-5300.